0026-895X/91/030440-06$03.00/0
Copyright © by The American Society for Pharmacology and Experimental Therapeutics
All rights of reproduction in any form reserved.
MOLECULAR PHARMACOLOGY, 40:440-445

MOL PHARM

Microsomal Reduction of 3-Amino-1,2,4-benzotriazine 1,4-Dioxide to a Free Radical

ROGER V. LLOYD,[1] DAVID R. DULING, GALINA V. RUMYANTSEVA, RONALD P. MASON, and PETER K. BRIDSON

Laboratory of Molecular Biophysics, National Institute of Environmental Health Sciences, Research Triangle Park, North Carolina 27709 (R.V.L., D.R.D., G.V.R., R.P.M.), and Department of Chemistry, Memphis State University, Memphis, Tennessee 38152 (P.K.B.)

Received February 14, 1991; Accepted May 30, 1991

SUMMARY

The drug SR 4233 (3-amino-1,2,4-benzotriazine 1,4-dioxide) is under pharmacological study as the lead compound in a new series of hypoxia-activated drugs, the benzotriazine *N*-oxides. However, the stable two- and four-electron-reduced metabolites of SR 4233, formed by the successive loss of the two oxygen atoms, are not pharmacologically active. In order to evaluate the possibility of an initial one-electron intermediate as the active species, we have used microsomal reduction and EPR spectroscopy to identify the first free radical reduction product. The unpaired electron is primarily centered on the 1-nitrogen, and the radical is best described as a nitroxide. Results with spin-trapping experiments show that reduction of SR 4233 to a free radical is followed by its air oxidation, resulting in the formation of the superoxide radical. Experiments with specific inhibitors suggest that the drug is being reduced by microsomal NADPH-cytochrome P-450 reductase.

The drug SR 4233 (3-amino-1,2,4-benzotriazine 1,4-dioxide) is the lead compound in a new series of hypoxia-activated drugs (Fig. 1), the benzotriazine *N*-oxides (1). It has a greater selective toxicity for hypoxic cells than drugs that are currently in use, including quinones and nitroimidazoles (2). Concentrations of SR 4233 up to 200 times greater are required to kill tumor cells *in vitro* under aerobic, compared with hypoxic, conditions. Such selectivity is important because hypoxic cells are resistant to radiation therapy.

The mode of action of many presently used anticancer drugs requires reductive metabolism, and SR 4233 is believed to act in the same manner (3). However, the first stable reduced metabolites of SR 4233 (3-amino-1,2,4-benzotriazine 1-oxide and 3-amino-1,2,4-benzotriazine; SR 4317 and SR 4330, respectively) (4), which are formed by the successive loss of the two oxygen atoms, are not themselves selective for hypoxic cells or even cytotoxic (5, 6). Therefore, it has been suggested that an intermediate one-electron reduction product (i.e., a free radical) is the active species (1, 6). Suggestions about the nature of the free radical have been made on a purely theoretical basis, but there has been no experimental evidence available that would lead to the identification, or even confirm the existence, of this free radical.

Microsomal enzymes are known to catalyze the anaerobic reduction of SR 4233 *in vitro*, and tumor tissues apparently can accomplish this *in vivo* (7). Therefore, we decided to investigate the formation of free radicals during the enzymatic reduction of SR 4233 catalyzed by rat liver microsomes, both by direct observation and by spin trapping.

Experimental Procedures

Samples of SR 4233 were supplied either by J. M. Brown of Stanford University or by the National Cancer Institute and were checked by mass spectrometry before use. SOD, NADPH, NADH, glucose-6-phosphate, glucose-6-phosphate dehydrogenase, *p*-hydroxymercuribenzoate, DTPA, and dicumarol were obtained from Sigma. Metyrapone (2-methyl-1,2-di-3-pyridyl-1-propanone) and DMPO were from Aldrich. The DMPO was vacuum-distilled and then stored at −70° until used. The catalase was from Boehringer-Mannheim and has been shown to be free of SOD contamination (8).

SR 4233 labeled with ^{15}N at the 2-nitrogen and the amino nitrogen was prepared from 2-nitroaniline and [^{15}N]cyanamide (universally labeled, 99% ^{15}N; ICON, Inc.) by the procedure of Mason and Tennant (9). The melting point of labeled SR 4317 was 278–281° (sealed tube; literature value, 275°). The melting point of labeled SR 4233 was 218° (literature value, 220°), and a mixed melting point with authentic nonlabeled material (National Cancer Institute) showed no change.

Experiments were run in a Tris buffer (150 mM KCl, 50 mM Tris·HCl, pH 7.36 at 25°) that was treated with Chelex ion exchange resin before use to remove adventitiously present metal ions. All chemicals were dissolved in the buffer (or minimal quantities of dimethyl sulfoxide, as was necessary for several of the inhibitors). Incubations consisted of microsomes homogenized in buffer (typically 3 mg of protein/ml), SR 4233 (4.2 mM), glucose-6-phosphate (type XXIII) (10

[1]Permanent address: Department of Chemistry, Memphis State University, Memphis, TN 38152.

ABBREVIATIONS: SOD, superoxide dismutase; DMPO, 5,5-dimethyl-1-pyrroline *N*-oxide; HFC, hyperfine coupling constant(s); DTPA, diethylenetriaminepentaacetic acid.

MOLECULAR PHARMACOLOGY
aspet
Downloaded from molpharm.aspetjournals.org at Universidade do Estado do Rio de Janeiro on December 4, 2012

mM) with glucose-6-phosphate dehydrogenase as an NADPH-generating system (10), and NADPH (1 mM). The rat liver microsomes were prepared by published methods and kept frozen at −70° until use (11). Buffer was added if necessary to maintain a constant total volume for all experiments. In all cases, the NADPH was added immediately before the EPR spectrum was taken.

For the inhibition experiments, specific inhibitors were added to the standard incubation. The effect of CO was studied by bubbling it through the incubation for 3 min before the addition of NADPH. In the spin-trapping experiments, DMPO was 100 mM, SOD either 50 or 250 μg/ml, catalase 1500 units/ml, and DTPA (as a chelator) 0.1 mM.

EPR observations were made at room temperature with a Varian E-109 or a Bruker ER-200 spectrometer equipped with a TM_{110} cavity. Samples were aspirated into a quartz flat cell by means of a rapid sampling device (Gilford Instruments) (12). When desired, spectra were accumulated for analysis with a Hewlett-Packard 9000 series computer. Oxygen consumption was determined with a Clark electrode (YSI-5331; Yellow Springs Instrument Company) in a water-jacketed cell held at 30°. The system was calibrated with a standard solution of sodium dithionite.

The EPR spectra were analyzed with the aid of computer fitting routines (13, 14) applied to the Fourier transforms of the experimental spectra. The Fourier transform of an EPR spectrum can be simulated with greater computational efficiency than the original spectrum. In addition, the number of observable lines in the spectrum is reduced, simplifying comparison between experimental and simulated spectra.

Results

The microsomal incubation of SR 4233 described above gave an EPR spectrum (Fig. 2A), after a brief induction period of 1–2 min that was required for the incubation to become anaerobic. After this, a steady state concentration was achieved, which was linearly proportional to the square root of the microsomal protein concentration ($r^2 = 0.978$; five points), indicating that radical decay was kinetically second-order (Fig. 3). This result implies nonenzymatic disproportionation or dimerization of the radical (15, 16). Computer analysis yielded the HFC and assignments listed in Table 1. The simulation based on these values, with an optimized Lorentzian linewidth of 1.0 G, is shown in Fig. 2B. In Fig. 2, C and D, the corresponding spectra for the ^{15}N-labeled compound are shown. The simulation in Fig. 2D is based on the HFC in Table 1, except that the two smaller nitrogen HFC values were converted to the corresponding values for ^{15}N. Simulations in which only one of the nitrogen HFC values was replaced by ^{15}N were not successful. With the omission of SR 4233 or NADPH from the incubation or with the use of heat-denatured microsomes, no EPR spectrum was observed (data not shown). SR 4317 examined under identical conditions did not give any EPR signal.

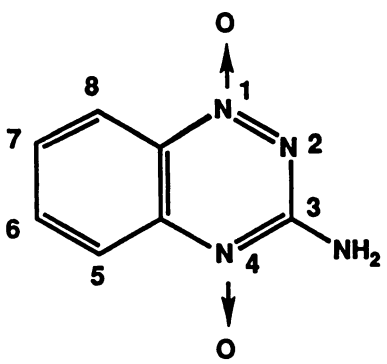

Fig. 1. Structure of SR 4233.

The effect of various known inhibitors of microsomal enzymes on the EPR signal intensity is shown in Table 2. The same cell remained in the cavity for the measurements on inhibitor and control solutions to minimize intensity differences due to cell position. The samples were then introduced by aspiration. Due to the extremely rapid rate of metabolism, an NADPH-generating system was necessary in addition to 1 mM NADPH, as evidenced by the diminished signal intensity in the absence of glucose-6-phosphate dehydrogenase.

The kinetics of oxygen consumption are shown in Fig. 4. There was no consumption in the absence of NADPH, and the basal oxygen consumption in the absence of SR 4233 was subtracted before analysis of the data. The Lineweaver-Burke plot (Fig. 4B) ($r^2 = 0.991$; seven points) gave $K_m = 1.4$ mM and $V_{max} = 0.9$ μmol of O_2/(min × mg of protein). Immediately after addition of catalase, there was a slight increase in oxygen concentration, followed by a decrease in oxygen consumption, suggesting that at least some of the oxygen consumed was converted to H_2O_2 (data not shown).

Incubations containing the spin trap DMPO gave the EPR spectrum shown in Fig. 5A. The observed spectrum is the sum of signals primarily from the DMPO-superoxide radical adduct, with a small signal from the DMPO-hydroxyl radical adduct. Assignments were made on the basis of known hyperfine splittings (17). Addition of SOD totally inhibited the formation of the DMPO-superoxide radical adduct and partially inhibited the formation of the DMPO-hydroxyl radical adduct (Fig. 5B), whereas catalase had no effect on the observed spectra (Fig. 5C). In the absence of SR 4233, there was only a weak background signal (Fig. 5D). The inhibition with SOD but not catalase shows that the hydroxyl radical adduct spectrum (Fig. 5B) is primarily an artifact due to the decomposition of the DMPO-superoxide radical adduct (18, 19), although the SOD-insensitive hydroxyl radical adduct may be formed by adventitious iron-reducing hydrogen peroxide (20).

Discussion

Laderoute *et al.* (21) have proposed, on theoretical grounds, that the one-electron reduction product is a carbon-centered radical protonated on the 4-oxygen (O-4), with the unpaired electron localized on the 3-carbon (C-3) because of the stabilizing effect of the amino group. The same carbon-centered radical has also been proposed for the metabolic reduction pathway (2, 5), although in fact the experimental evidence did not implicate any specific radical. The large nitrogen HFC that we observe (11.5 G) is in the expected range for a nitrogen-centered free radical, such as a nitroxide, rather than for the amino-substituted carbon radical that would result if the radical site were actually localized on C-3. The two small nitrogen HFC observed in the spectrum are both substituted by ^{15}N in the spectrum of the labeled compound. From the reaction used for the synthesis, the ^{15}N atoms, and, therefore, the two small nitrogen HFC, are unequivocally from N-2 and the NH_2 group. We assign the smaller nitrogen HFC (2.98 G) and the nearly identical proton HFC (2.95 G, two equivalent protons) to the amino group. The remaining nitrogen HFC is due to N-2, and the larger proton HFC arise from the ring protons *ortho-para* to the radical nitrogen. The question of whether the 11.5 G nitrogen HFC arises from N-1 or N-4 is discussed below.

The mechanism shown in Fig. 6 proposes a radical delocalized over atoms 1–3, with the unpaired spin density primarily on

MOL PHARM
MOLECULAR PHARMACOLOGY
aspet
Downloaded from molpharm.aspetjournals.org at Universidade do Estado do Rio de Janeiro on December 4, 2012

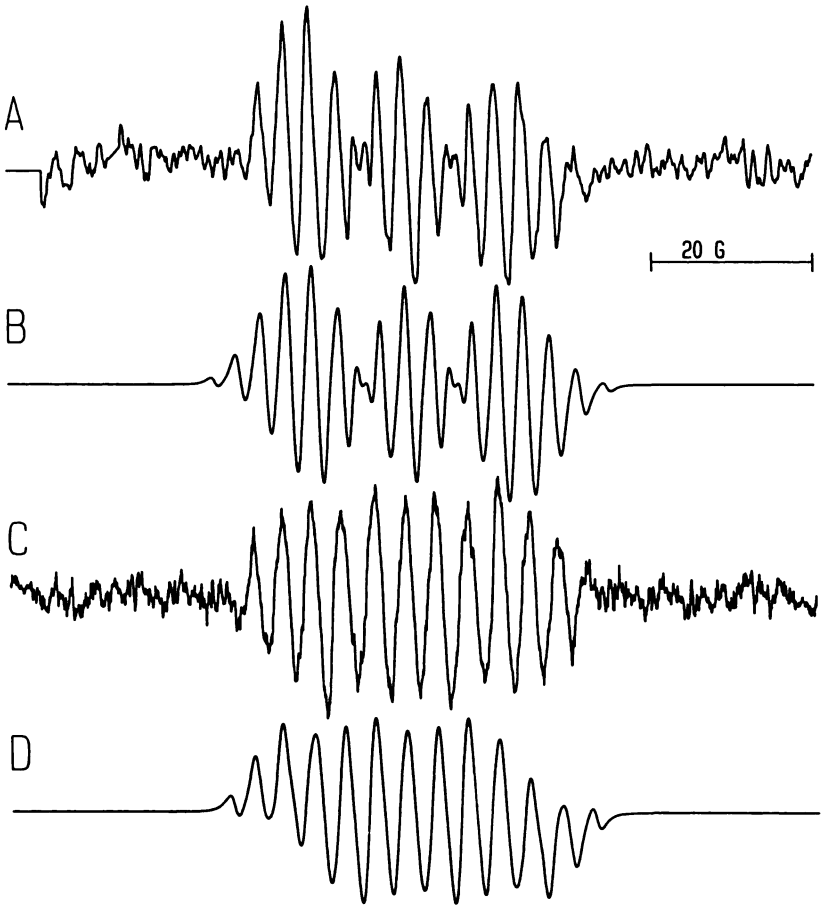

Fig. 2. A, First-derivative EPR spectrum obtained by microsomal reduction of SR 4233. Incubation: rat liver microsomes, approximately 3 mg of protein/ml; SR 4233, 4.23 mM; glucose-6-phosphate, 10 mM; glucose-6-phosphate dehydrogenase, 13 units/ml; NADPH, 1 mM. Instrumental parameters: sweep width, 100 G; modulation amplitude, 0.8 G; time constant, 330 msec; microwave power, 20 mW. B, Computer simulation of spectrum in A, based on the HFC listed in Table 1 and an optimized Lorentzian linewidth of 1.0 G. C, Experimental spectrum from reduction of SR 4233 labeled with ^{15}N at N-2 and N-NH_2. D, Simulation of spectrum in C, based on the parameters of Table 1, with the ^{15}N values used.

N-1 and its attached oxygen. Protonation of the oxygen on N-4 with a pK_a of 6.0 (21) is then followed by another one-electron reduction, through the second-order disproportionation and concomitant loss of hydroxide ion, to give the two-electron reduction product, with $2k_d \simeq 3 \times 10^7$ M^{-1} sec^{-1} (21), in agreement with our observed second-order decay kinetics (Fig. 7).

Effectively, there is a two-electron reduction of the ring together with a one-electron oxidation of the *N*-oxide at N-1 to a nitroxide radical, resulting in a net one-electron reduction. These schemes are consistent with the fact that the first stable reduction product of SR 4233 is the 1-oxide, formed by removal of the oxygen on N-4, and with our observation that in the EPR spectrum there is only one large nitrogen HFC. It differs from those previously proposed in that the radical is formulated as a nitroxide at N-1 with some electron delocalization over N-1 to C-3, rather than a carbon-centered radical localized on C-3.

Calculations on the anion radical of SR 4233 with the AM1 Hamiltonian in the MOPAC semiempirical program (22) show the unpaired electron π orbital spin density primarily on N-1 (0.28) and O-1 (0.23), instead of N-4 (0.06) or C-3 (0.09), which is consistent with unpaired electron distributions calculated for nitroxide radicals (23). The results of the calculations and the observed large nitrogen HFC are both in agreement with previous studies on amine *N*-oxide anion radicals (24, 25), but we believe that identification of the radical as a nitroxide is more reasonable.

The small HFC observed for the amino group, implying only a small interaction with the unpaired electron, is consistent with a comparison of the structure-activity relationships observed for SR 4233 and SR 4482 (1,2,4-benzotriazine 1,4-dioxide) (1). The latter differs from SR 4233 only in the lack of the amino group and was the only drug of 16 SR 4233 analogs tested that was found to be more toxic to hypoxic cells *in vitro* than SR 4233 itself, indicating that the amino group is not physiologically important.

CO and metyrapone are specific inhibitors of the cytochrome P-450 electron-transport system (26), and the absence of any effect on the EPR signal suggests that at most only a small fraction of the SR 4233 is being reduced by this cytochrome. The dependence of radical formation on NADPH and an NADPH-generating system is consistent with NADPH-cytochrome P-450 reductase being the site of electron transfer. This conclusion is supported by the observed effect of *p*-hydroxymercuribenzoate, a known inhibitor of NADPH-dependent electron transport in liver microsomes (27). The lack of effect of dicumarol shows that microsomal DT-diaphorase is not involved (27). The results of the DMPO spin trap experiments indicate that the one-electron reduction of SR 4233 to a nitroxide radical is followed by its air oxidation, resulting in the formation of superoxide radical by electron transfer. The enzymatic reduction of di-*N*-oxides to free radical metabolites is widely distributed among flavoenzymes (28). Presumably, all di-*N*-oxide reductases that appear to show oxygen inhibition form the oxygen-sensitive free radical as an obligate intermediate.

Recently, the anerobic microsomal reduction of SR 4233 to

MOL PHARM
MOLECULAR PHARMACOLOGY
aspet
Downloaded from molpharm.aspetjournals.org at Universidade do Estado do Rio de Janeiro on December 4, 2012

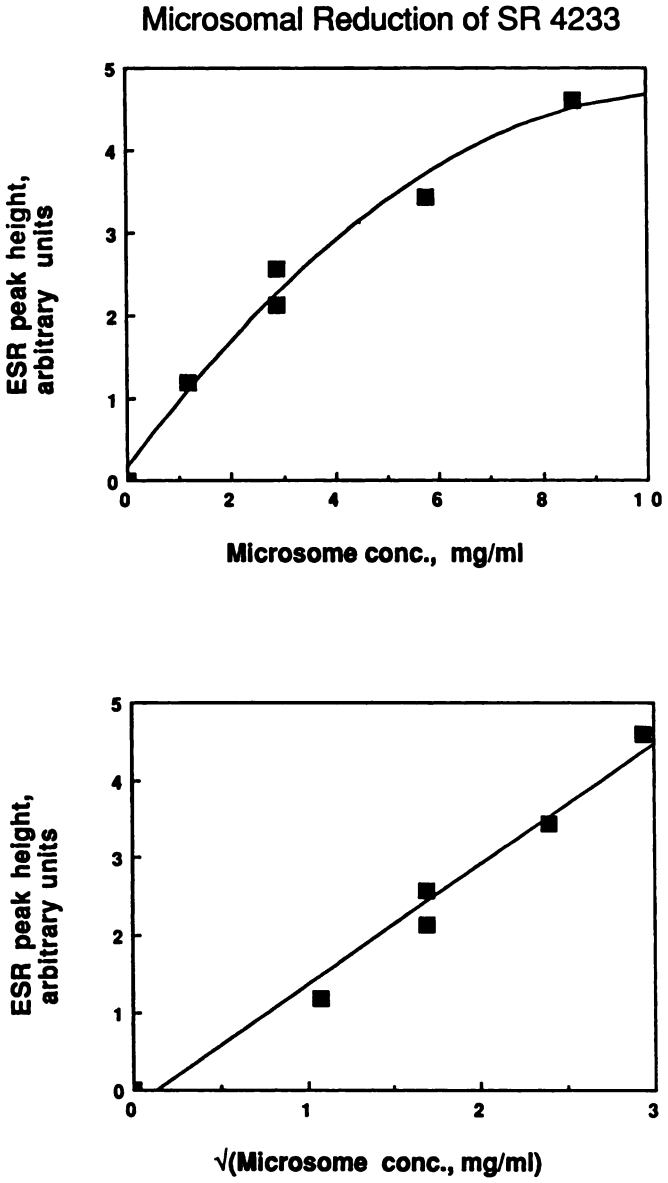

Fig. 3. Effect of microsome concentration on the intensity of the EPR signal from SR 4233. *Upper*, microsome concentration (mg of protein/ml) versus EPR signal intensity (arbitrary units). *Lower*, square root of microsome concentration versus EPR signal intensity (arbitrary units).

TABLE 1

ESR HFC for the radical from SR 4233, obtained by computer simulation of the Fourier transform of the observed spectrum

Nucleus	HFC
	G
N-1	11.50
N-2	3.38 (^{15}N, 4.47)
N-NH_2	2.98 (^{15}N, 4.11)
H-ring	3.53 (2)
H-NH_2	2.95 (2)

TABLE 2

Relative intensities of ESR spectra of the SR 4233 radical

Inhibitor	Relative amplitude[a]
Control (standard incubation)[b]	100
+CO	98 ± 5
+Metyrapone (1.0 mM)	100 ± 6
+Dicumarol (0.1 mM)	96 ± 5
−Dehydrogenase	42 ± 14
+*p*-Hydroxymercuribenzoate (0.5 mM)	0

[a] The effect of each inhibitor was compared with its own control, e.g., a 100% CO atmosphere was compared with a 100% nitrogen atmosphere. The errors are standard error (three experiments).

[b] Each 2-ml incubation contained rat liver microsomes (approximately 5 mg/ml), SR 4233 (4.5 mM), glucose-6-phosphate (10 mM), glucose-6-phosphate dehydrogenase (10 units/ml), and NADPH (1 mM).

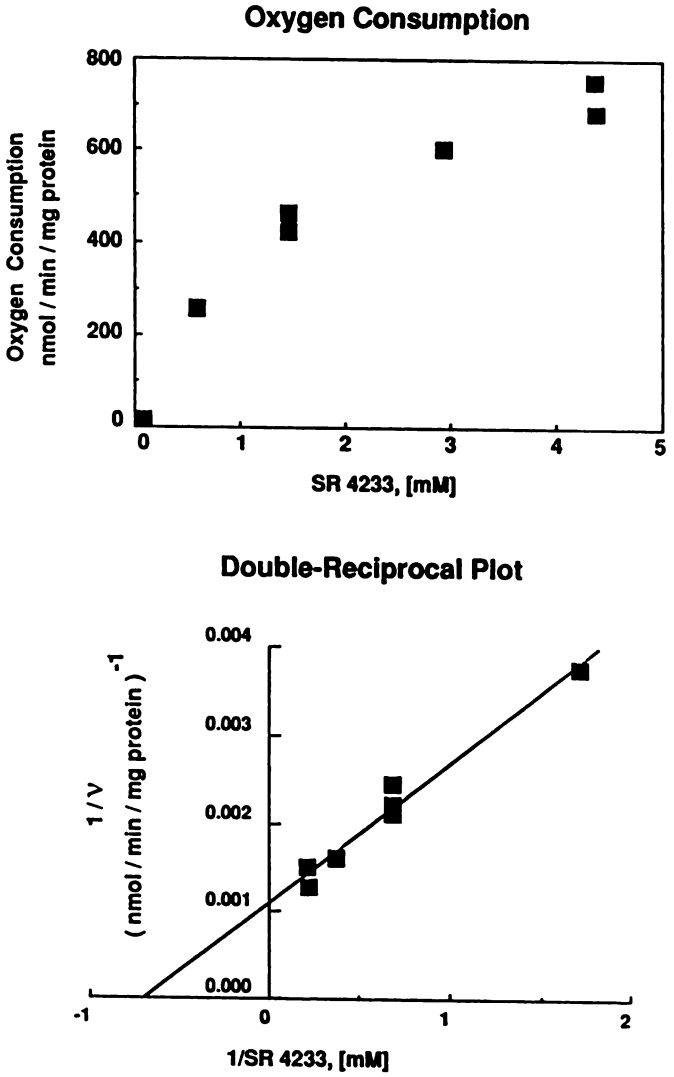

Fig. 4. Kinetics of oxygen consumption by the reduction of SR 4233. The standard incubation was used (see Fig. 1). *Upper*, concentration of SR 4233 versus rate of oxygen consumption. *Lower*, double-reciprocal (Lineweaver-Burke) plot for oxygen consumption.

its two-electron reduction product SR 4317 was reported to have a K_m of 1.4 mM and a V_{max} of 950 nmol/min/mg of protein (28). These values are in excellent agreement with the K_m (1.4 mM) and V_{max} (900 nmol/min/mg of protein) that we determined for futile cycling due to radical metabolite formation, and they further support the proposal that SR 4317 formation is due to nonenzymatic disproportionation of the SR 4233 nitroxide radical metabolite (Fig. 7). In contrast to radical formation, SR 4317 formation was reported to be strongly inhibited by CO. This result is hard to understand, in view of the high V_{max} reported for this reduction (28), which is typical

MOL PHARM
MOLECULAR PHARMACOLOGY
aspet
Downloaded from molpharm.aspetjournals.org at Universidade do Estado do Rio de Janeiro on December 4, 2012

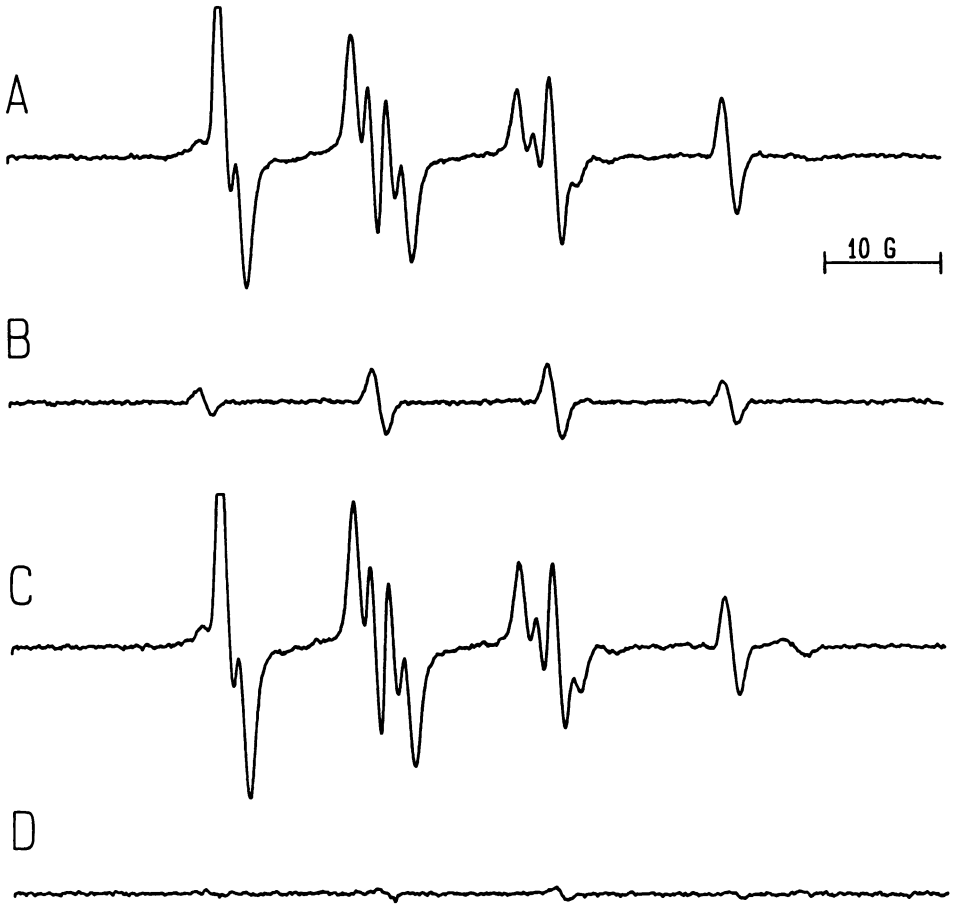

Fig. 5. A, EPR spectrum from the standard incubation (see Fig. 1) plus the spin trap DMPO (100 mM). B, Standard incubation plus DMPO and SOD (200 μg/ml). C, Standard incubation plus DMPO and catalase (100 μg/ml). D, Standard incubation plus DMPO minus SR 4233.

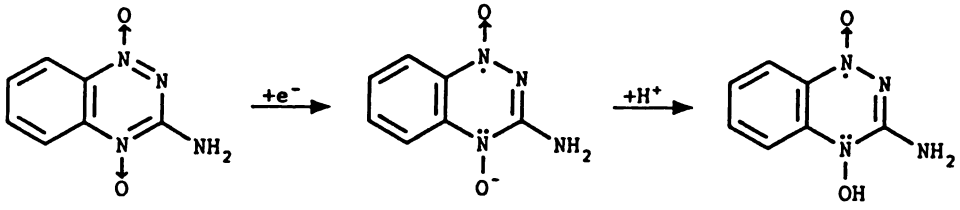

Fig. 6. Proposed scheme for radical formation.

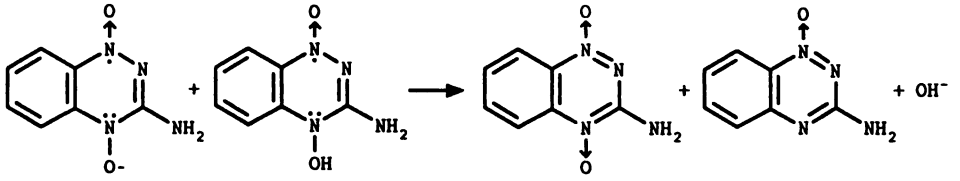

SR 4233 SR 4317

Fig. 7. Proposed scheme for formation of two-electron reduction product.

of NADPH-cytochrome P-450 reductase (29, 30) but unusually high for cytochrome P-450.

Acknowledgments

We thank Dr. J. M. Brown and the Drug Synthesis and Chemistry Branch, Division of Cancer Treatment, National Cancer Institute, for providing us with samples of SR 4233.

References

1. Zeman, E. M., M. A. Baker, M. J. Lemmon, C. I. Pearson, J. A. Adams, J. M. Brown, W. W. Lee, and M. Tracy. Structure-activity relationships for benzotriazine di-*N*-oxides. *Int. J. Radiat. Oncol. Biol. Phys.* **16**:977–981 (1989).
2. Costa, A. K., M. A. Baker, J. M. Brown, and J. R. Trudell. *In vitro* hepatotoxicity of SR 4233 (3-amino-1,2,4-benzotriazine-1,4-dioxide), a hypoxic cytotoxin and potential antitumor agent. *Cancer Res.* **49**:925–929 (1989).
3. Zeman, E. M., V. K. Hirst, M. J. Lemmon, and J. M. Brown. Enhancement of radiation-induced tumor cell killing by the hypoxic cell toxin SR 4233. *Radiother. Oncol.* **12**:209–218 (1988).
4. Laderoute, K. R., and A. M. Rauth. Identification of two major reduction products of the hypoxic cell toxin 3-amino-1,2,4-benzotriazine-1,4-dioxide. *Biochem. Pharmacol.* **35**:3417–3420 (1986).
5. Baker, M. A., E. M. Zeman, V. K. Hirst, and J. M. Brown. Metabolism of SR 4233 by Chinese hamster ovary cells: basis of selective hypoxic cytotoxicity. *Cancer Res.* **48**:5947–5952 (1988).
6. Zeman, E. M., J. M. Brown, M. J. Lemmon, V. K. Hirst, and W. W. Lee. SR 4233: A new bioreductive agent with high selective toxicity for hypoxic mammalian cells. *Int. J. Radiat. Oncol. Biol. Phys.* **12**:1239–1242 (1986).
7. Walton, M. I., and P. Workman. High-performance liquid chromatographic assay for the benzotriazine di-*N*-oxide (SR 4233) and its reduced metabolites in biological materials. *J. Chromatogr.* **430**:429–437 (1988).
8. Halliwell, B. Superoxide dismutase: a contaminant of bovine catalase. *Biochem. J.* **135**:379–381 (1973).

MOL PHARM
MOLECULAR PHARMACOLOGY
aspet
Downloaded from molpharm.aspetjournals.org at Universidade do Estado do Rio de Janeiro on December 4, 2012

9. Mason, J. C., and G. Tennant. Heterocyclic *N*-oxides. VI. Synthesis and nuclear magnetic resonance spectra of 3-aminobenzo-1,2,4-triazines and their mono- and di-*N*-oxides. *J. Chem. Soc.* Sect. B 911–916 (1970).
10. Mason, R. P., and J. L. Holtzman. The mechanism of microsomal and mitochondrial nitroreductase: electron spin resonance evidence for nitroaromatic free radical intermediates. *Biochemistry* **14**:1626–1632 (1975).
11. Docampo, R., R. P. Mason, C. Mottley, and R. P. A. Muniz. Generation of free radicals induced by nifurtimox in mammalian tissues. *J. Biol. Chem.* **256**:10930–10933 (1981).
12. Mason, R. P. Assay of *in situ* radicals by electron spin resonance. *Methods Enzymol.* **105**:416–422 (1984).
13. Duling, D. R., A. G. Motten, and R. P. Mason. Generation and evaluation of isotropic ESR spectrum simulations. *J. Magn. Reson.* **77**:504–511 (1988).
14. Motten, A., and J. Schreiber. Correlation analysis of ESR spectra on a small computer. *J. Magn. Reson.* **67**:42–54 (1986).
15. Yamazaki, I., and L. H. Piette. Mechanism of free radical formation and disappearance during the ascorbic acid oxidase and peroxidase reactions. *Biochem. Biophys. Acta* **50**:62–69 (1961).
16. Docampo, R., S. N. J. Moreno, and R. P. Mason. Generation of free radical metabolites and superoxide anion by the calcium indicators arsenazo III, antipyrylazo III, and murexide in rat liver microsomes. *J. Biol. Chem.* **258**:14920–14925 (1983).
17. Li, A. S. W., K. B. Cummings, H. P. Roethling, G. R. Buettner, and C. F. Chignell. A spin-trapping database implemented on the IBM PC/AT. *J. Magn. Reson.* **79**:140–142 (1988).
18. Finkelstein, E., G. M. Rosen, E. J. Rauckman, and J. Paxton. Spin trapping of superoxide. *Mol. Pharmacol.* **16**:676–685 (1979).
19. Finkelstein, E., G. M. Rosen, and E. J. Rauckman. Production of hydroxyl radical by decomposition of superoxide spin-trapped adducts. *Mol. Pharmacol.* **21**:262–265 (1982).
20. Kalyanaraman, B., K. M. Morehouse, and R. P. Mason. An electron paramagnetic resonance study of the interactions between the Adriamycin semiquinone, hydrogen peroxide, iron-chelators, and radical scavengers. *Arch. Biochem. Biophys.* **286**:164–170 (1991).
21. Laderoute, K., P. Wardman, and A. M. Rauth. Molecular mechanisms for the hypoxia-dependent activation of 3-amino-1,2,4-benzotriazine-1,4-dioxide (SR 4233). *Biochem. Pharmacol.* **37**:1487–1495 (1988).
22. Stewart, J. J. P. QCPE Program 455, version 5.0 (1989).
23. Davis, T. D., R. E. Christofferson, and G. M. Maggiora. *Ab initio* calculations on large molecules using molecular fragments. *J. Am. Chem. Soc.* **97**:1347–1354 (1975).
24. Kubota, T., K. Nishikida, H. Miyazaki, K. Iwatani, and Y. Oishi. Electron spin resonance and polarographic studies of the anion radicals of heterocyclic amine *N*-oxides. *J. Am. Chem. Soc.* **90**:5080–5090 (1968).
25. Gamba, A., V. Malatesta, G. Morosi, C. Oliva, and M. Simonetta. Ultraviolet and electron spin resonance spectra of nitropyridines and nitropyridine *N*-oxides. *J. Phys. Chem.* **77**:2744–2752 (1973).
26. Ernster, L., and K. Nordenbrand. Microsomal lipid peroxidation. *Methods Enzymol.* **10**:574–580 (1967).
27. Ernster, L., and S. Orrenius. Substrate-induced synthesis of the hydroxylating enzyme system of liver microsomes. *Fed. Proc.* **24**:1190–1199 (1965).
28. Walton, M. I., and P. Workman. Enzymology of the reductive bioactivation of SR 4233: a novel benzotriazine di-*N*-oxide hypoxic cell cytotoxin. *Biochem. Pharmacol.* **39**:1735–1742 (1990).
29. Cummings, S. W., B. B. Curtis II, J. A. Peterson, and R. A. Prough. The effect of the *tert*-butylquinone metabolite of butylated hydroxyanisole on cytochrome P-450 monooxygenase activity. *Xenobiotica* **20**:915–924 (1990).
30. Yasukochi, Y., and B. S. S. Masters. Some properties of a detergent-solubilized NADPH-cytochrome *c* (cytochrome P-450) reductase purified by biospecific affinity chromatography. *J. Biol. Chem.* **251**:5337–5344 (1976).

Send reprint requests to: Dr. Ronald P. Mason, NIEHS, P.O. Box 12233, Research Triangle Park, NC 27709.

MOL PHARM
MOLECULAR PHARMACOLOGY
aspet
Downloaded from molpharm.aspetjournals.org at Universidade do Estado do Rio de Janeiro on December 4, 2012